

Theory of two-photon double ionization of helium at the sequential threshold

H. Bachau*

Centre des Lasers Intenses et Applications, Université Bordeaux I–CNRS-CEA, 33405 Talence Cedex, France

(Received 8 December 2010; published 9 March 2011)

We analyze in this paper the process of double-electron ejection through two-photon absorption from the fundamental state of helium. We focus on the case of photon energies close to 2 a.u., which marks the threshold between direct and sequential double-ionization regimes. We demonstrate the crucial role of two-photon excitation-plus-ionization process of $nlk'l'$ Rydberg series. We show that the latter channel must be taken into account in the theory in order to properly describe two-electron ejection. A simple expression is derived for the electron energy spectrum, leading to better insights into the physics underlying two-photon absorption close to the sequential threshold.

DOI: [10.1103/PhysRevA.83.033403](https://doi.org/10.1103/PhysRevA.83.033403)

PACS number(s): 32.80.Rm, 32.80.Ee, 32.80.Fb

I. INTRODUCTION

During recent years, there has been tremendous activity in investigations of helium two-photon double ionization (TPDI). In helium the ionization potential for double ionization is about 2.903 a.u.; therefore TPDI is energetically forbidden for photon energies lower than 1.45 a.u. (39.5 eV). If we consider a long pulse duration and a relatively low intensity (such that three-photon double ionization can be neglected) TPDI is a direct process for photon energies lower than 2 a.u. (54.42 eV) while it is dominated by sequential ionization for larger photon energies [1]. In the latter case the helium atom is first ionized; in a second step the residual ion, He^+ , is also ionized. The electrons in the double continuum share the excess energy E_{exc} ($E_{\text{exc}} = -2.903 + 2\hbar\omega$). Despite the efforts of theoreticians, many problems remain to be resolved, in particular in the direct regime. For example, cross sections reported in different publications do not agree, and neither do the photoelectron energy distributions [2]. In addition to these discrepancies between theoretical results, there is a new issue, namely, the sharp rise of the TPDI cross section around 2 a.u. [3–8], that is the subject of ongoing debates [9]. This brings our attention to TPDI in the threshold region of the sequential process, i.e., at photon energies close to 2 a.u. As far as we know, TPDI has not been thoroughly investigated in this region, at least from the formal point of view. The purpose of this paper is to report on TPDI theory in the threshold region of the sequential process.

We have noticed above that, for photon energies larger than 2 a.u., sequential ionization dominates. The natural continuation of the double ionization channel below threshold is the excitation-plus-ionization channel, where one of the electrons is expected to be in a Rydberg state, while the other is in the continuum; see Fig. 1. When the photon energy is lower but close to 2 a.u., the latter channel is expected to play an important role. To be more specific, one must investigate both $nlk'l'$ and $klk'l'$ series of states (which are related to excitation-plus-ionization and double-ionization channels, respectively) populated through two-photon absorption. It is easy to understand that solving the time-dependent Schrödinger equation (TDSE) would lead to tremendous difficulties in the present context. Indeed, TDSE methods involve in general a radial “box,” of fixed dimension, or expansions over L^2

functions, limiting the number of nl Rydberg states taken into account ($n < n_{\text{max}}$). Furthermore, the TDSE also implies a laser pulse of given duration, with laser bandwidth effects complicating the problem [9]. Here we reconsider an approach developed some years ago, based on the resolvent operator formalism [1]. The atomic structure is represented using a zero-order representation (in $1/Z$) in perturbation theory while the treatment of the laser-atom interaction includes all photoabsorption processes up to two-photon absorption. These approximations have been thoroughly discussed in our previous paper. Although crude, the representation of the atomic structure is not unphysical since electron correlations are not required for TPDI to occur, in contrast to one-photon double ionization. Also, the resolvent operator method is suitable to explore the limit of laser pulse of infinite duration, getting rid of laser bandwidth effects. As we shall see below, the approach provides clear physical insights into the dominant physical mechanisms underlying the TPDI process. The theoretical approach and its application are presented in the following section. The resolvent operator technique has been extensively used in the past and we only present the main steps of the development; details can be found in [10,11]. We provide a simple expression of the electron energy spectrum in the region close to threshold. The conclusion is given in the last section.

Atomic units are used unless otherwise stated.

II. FORMALISM AND APPLICATIONS

A. Theoretical approach

In order to derive an expression for the photoelectron energy spectrum, we consider $|1s^2\rangle$ as the initial atomic state, in the presence of the field represented by photon number state $|N\rangle$. The interacting system “atom + field” will be denoted by $|I\rangle = |1s^2\rangle|N\rangle$. The intermediate states $|1sk'l'\rangle$, populated through one-photon absorption from $|1s^2\rangle$, are denoted by $|C\rangle = |1sk'l'\rangle|N-1\rangle$. The final double-continuum states $|klk'l'\rangle$, produced through two-photon absorption, are denoted by $|F\rangle = |klk'l'\rangle|N-2\rangle$. As explained in the Introduction, we must also include the Rydberg series of states $|nlk'l'\rangle$, denoted by $|R\rangle = |nlk'l'\rangle|N-2\rangle$, in our treatment. The energy of state $|I\rangle$ is given by $E_I = E_{1s^2} + N\omega$. In zero order of perturbation theory $E_{1s^2} = 2E_{1s} + \langle 1s^2|1/r_{12}|1s^2\rangle$, E_{1s} being the energy of the $1s$ orbital of He^+ . Note that, during the ionization of He, the electron interaction energy $\langle 1s^2|1/r_{12}|1s^2\rangle$ is transferred to the ionized electron and transformed into

*bachau@celia.u-bordeaux1.fr

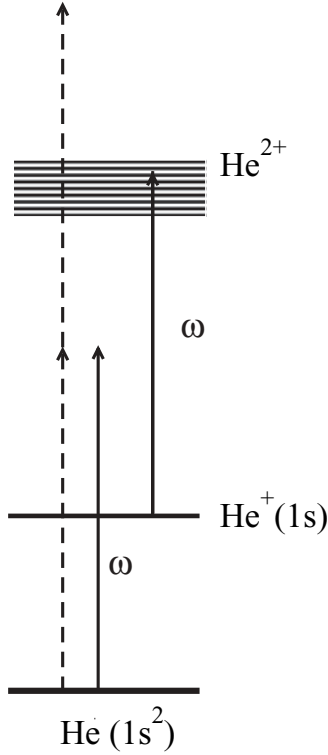


FIG. 1. A schematic diagram of the levels involved in two-photon absorption for a photon energy slightly below 2. Two-electron ejection is a direct process (vertical dashed arrows) while sequential absorption (vertical full arrows) populates the He continuum and He⁺ Rydberg states. The series of thin horizontal lines below He²⁺ represents He⁺ Rydberg states (not at scale) converging to the He double ionization threshold.

kinetic energy. The energy of the other states, $|1skl\rangle$, $|klk'l'\rangle$, and $|nlk'l'\rangle$, are given by the sum of the corresponding hydrogenic orbital energies, calculated for $Z = 2$. Therefore the energies of states $|C\rangle$, $|F\rangle$, and $|R\rangle$ are given by $E_C = E_{1s} + E_{k'l'} + (N - 1)\omega$, $E_F = E_{kl} + E_{k'l'} + (N - 2)\omega$, and $E_R = E_{nl} + E_{k'l'} + (N - 2)\omega$, respectively. Note that, within the lowest-order perturbation theory (LOPT), $l = l' = 1$. Denoting as V the dipole interaction between atom and field, the resolvent operator approach leads to the set of equations [1]

$$(z - \omega_I)G_{II} = 1 + \int_C V_{IC}G_{CI}, \quad (1)$$

$$(z - \omega_C)G_{CI} = V_{CI}G_{II} + \int_F V_{CF}G_{FI} + \sum_R V_{CR}G_{RI}, \quad (2)$$

$$(z - \omega_F)G_{FI} = \int_C V_{FC}G_{CI}, \quad (3)$$

$$(z - \omega_R)G_{RI} = \int_C V_{RC}G_{CI}. \quad (4)$$

Using Eqs. (3) and (4) with Eq. (2) we obtain

$$(z - \omega_C)G_{CI} = V_{CI}G_{II} + \int_F \frac{|V_{CF}|^2}{z - \omega_F} G_{CI} + \sum_R \frac{|V_{CR}|^2}{z - \omega_R} G_{CI}. \quad (5)$$

In the following we assume that the continuum states are normalized on the energy scale.

B. The sequential regime ($\omega > 2$)

Following the standard procedure, we set $z = \omega_C + i\eta$ in the denominators of the right-hand-side term $\int_F \frac{|V_{CF}|^2}{z - \omega_F} G_{CI}$, in Eq. (5), and we calculate the limit $\eta \rightarrow 0^+$. The integral over F separates into a real and an imaginary part, the first leading to a shift and the second to the width of state C . It has the expression

$$\gamma_C = \gamma_{\text{He}^+} = 2\pi |\langle kl|\mu|1s\rangle|^2 \quad (6)$$

with $E_k = E_{1s} + \omega$ (E_k denotes E_{kl}); μ is the dipole coupling. The term $\sum_R \frac{|V_{CR}|^2}{\omega_C - \omega_R} G_{CI}$ has no pole in the denominator; it is real and it corresponds to a shift. Neglecting the shifts, Eq. (2) now reads

$$(z - \omega_C + \frac{1}{2}i\gamma_C)G_{CI} = V_{CI}G_{II}. \quad (7)$$

Similarly to Eq. (2), we introduce the width of state I in Eq. (1):

$$(z - \omega_I + \frac{1}{2}i\gamma_I)G_{II} = 1 \quad (8)$$

with

$$\gamma_I = \gamma_{\text{He}} = 2\pi |\langle 1sk'l'|\mu|1s^2\rangle|^2 \quad (9)$$

and $E_{k'} = E_{1s^2} + \omega - E_{1s}$. Now, using the above equations for G_{II} and G_{CI} , we express G_{FI} as

$$G_{FI} = \frac{V_{FC}V_{CI}}{(z - \omega_F)(z - \omega_C + \frac{1}{2}i\gamma_C)(z - \omega_I + \frac{1}{2}i\gamma_I)} \quad (10)$$

or

$$G_{FI} = \frac{V_{FC}V_{CI}}{(z - z_1)(z - z_2)(z - z_3)} \quad (11)$$

with $z_1 = \omega_F$, $z_2 = \omega_C - \frac{1}{2}i\gamma_C$, and $z_3 = \omega_I - \frac{1}{2}i\gamma_I$. The two-photon transition amplitude $U_{FI}(T)$ is obtained as the inverse Laplace transform of $G_{FI}(z)$; at the end of the laser pulse (i.e., at time T), it reads

$$U_{FI}(T) = V_{FC}V_{CI} \left[\frac{e^{-iz_1T}}{(z_1 - z_2)(z_1 - z_3)} + \frac{e^{-iz_2T}}{(z_2 - z_1)(z_2 - z_3)} + \frac{e^{-iz_3T}}{(z_3 - z_2)(z_3 - z_1)} \right]. \quad (12)$$

The photoelectron spectrum corresponds to the spectrum of final states of the two-photon two-electron transition; it is given by $\lim_{T \rightarrow \infty} |U_{FI}(T)|^2$. In the above expression, two of the three exponentials (i.e., the two last ones) decay as $T \rightarrow \infty$. Finally, after some straightforward algebraic manipulation, the

transition amplitude is written as

$$U_{k,k'}^{(2)}(T \rightarrow \infty) = \frac{\langle 1sk'l'|\mu|1s^2\rangle\langle kl|\mu|1s\rangle}{\{[E_k + E_{k'} - (E_{1s^2} + 2\omega)] + \frac{1}{2}i\gamma_{\text{He}}\}\{[E_k - (E_{1s} + \omega)] + \frac{1}{2}i\gamma_{\text{He}^+}\}}. \quad (13)$$

Taking into account antisymmetrized states and all channels leading to double ionization, the resulting one-electron energy spectrum given by

$$\frac{dP_k}{dk} = \frac{1}{2} \int_{E_{k'}} dE_{k'} |U_{k,k'}^{(2)}(T \rightarrow \infty) + U_{k',k}^{(2)}(T \rightarrow \infty)|^2 \quad (14)$$

is dominated by two peaks, centered at energies $E_1 = E_{1s^2} + \omega - E_{1s}$ and $E_2 = E_{1s} + \omega$. In the resonance regions

$$|\tilde{U}_{k,k'}^{(2)}(T \rightarrow \infty)|^2 = \frac{1}{4\pi^2} \frac{\gamma_{\text{He}}\gamma_{\text{He}^+}}{[(E_k + E_{k'} - E_{1s^2} - 2\omega)^2 + \frac{1}{4}\gamma_{\text{He}}^2][(E_k - E_{1s} - \omega)^2 + \frac{1}{4}\gamma_{\text{He}^+}^2]}. \quad (16)$$

Figure 2 shows the electron energy spectrum calculated for $\omega = 2.1$. It is based on realistic values of the ionization rates of He and He⁺, 0.066 and 0.061, respectively. These rates have been calculated for an intensity of 0.1 (14.04×10^{15} W/cm²). This rather large value has been chosen for the sake of clarity in Fig. 2, a smaller intensity resulting in narrower (and higher) peaks. We recognize the two structures, at the expected positions. It is worth recalling that the peaks have unequal heights and that their widths are the result of a convolution, and not from a simple Lorentzian.

C. The direct regime ($\omega < 2$)

We focus on Eq. (5); the term $\int_F \frac{|V_{CF}|^2}{z - \omega_F} G_{CI}$ has no pole, it is real, and it corresponds to a shift. On the other hand, the term $\sum_R \frac{|V_{CR}|^2}{z - \omega_R} G_{CI}$ now has a pole, associated with a resonant (or

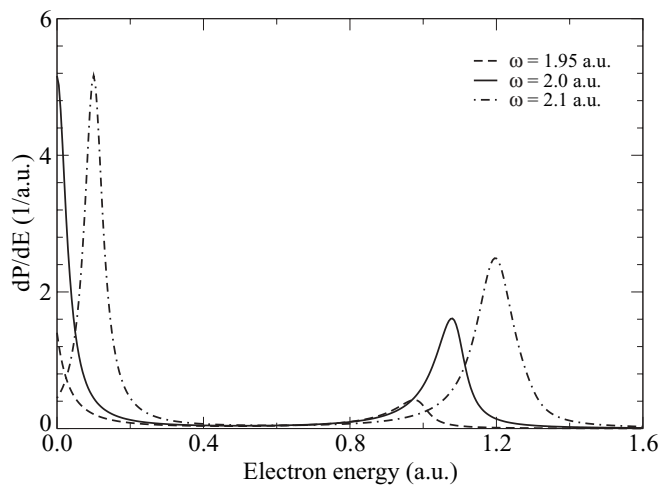


FIG. 2. TPDI one-electron energy spectrum calculated for three photon energies, given in the figure. The equation (15) is used with $\gamma_{\text{He}} = 0.066$ and $\gamma_{\text{He}^+} = \gamma_R = 0.061$.

the interference term plays a negligible role in the above expression. Therefore, around the peaks

$$\frac{dP_k}{dk} \approx \frac{1}{2} \int_{E_{k'}} dE_{k'} [|\tilde{U}_{k,k'}^{(2)}(T \rightarrow \infty)|^2 + |\tilde{U}_{k',k}^{(2)}(T \rightarrow \infty)|^2], \quad (15)$$

with

quasiresonant) coupling between the $1s$ state and a Rydberg state nl ($E_{1s} + \omega \simeq E_{nl}$). Considering the latter case, in the limit of high-lying Rydberg series the discrete summation over R in the right-hand side of Eq. (5) is written

$$\sum_R \frac{|V_{CR}|^2}{z - \omega_R} G_{CI} \approx \int_R \frac{dE_R}{\Delta E_R} \frac{|V_{CR}|^2}{z - \omega_R} G_{CI} \quad (17)$$

with $\Delta E_R = \frac{Z^2}{n^3}$, that is, the spacing between Rydberg states, and $Z = 2$. In the above expression, we have simply transformed a discrete summation into an integral one by introducing the density of energy $1/\Delta E_R$. Following the procedure previously explained, the integration over R separates into a real and an imaginary part. The latter contribution corresponds to a width, given by

$$\gamma_R = 2\pi \frac{1}{\Delta E_R} |\langle nl|\mu|1s\rangle|^2 \quad (18)$$

with $E_{nl} \simeq E_{1s} + \omega$. It is important to notice that this procedure is valid provided that $\gamma_R \gg \Delta E_R$; in other cases γ_R is not defined. Here we do not consider the particular problem of core resonances, where the $1s$ state of He⁺ is resonantly coupled to an isolated He⁺ nl state. It is well known that core resonances strongly perturb two-photon single-ionization cross sections, but there is no evidence that they also affect TPDI; the problem remains open [4] and is out of the scope of the present paper. Here, the He⁺($1s$) state “decays” to a dense He⁺(nl) Rydberg series, with a rate γ_R . This problem has similarities with a discrete state coupled to a discretized continuum (a detailed development of which may be found in Cohen-Tannoudji *et al.* [12], Chap. I; see also [13], Appendix B). Following the development leading to Eq. (10), G_{FI} now reads

$$G_{FI} = \frac{V_{FC}V_{CI}}{(z - \omega_F)(z - \omega_C + \frac{1}{2}i\gamma_R)(z - \omega_I + \frac{1}{2}i\gamma_I)}. \quad (19)$$

The transition amplitude is given by

$$U_{k,k'}^{(2)}(T \rightarrow \infty) = \frac{\langle 1s k'l' | \mu | 1s^2 \rangle \langle kl | \mu | 1s \rangle}{\{[E_k + E_{k'} - (E_{1s^2} + 2\omega)] + \frac{1}{2}i\gamma_{\text{He}}\} \{[E_k - (E_{1s} + \omega)] + \frac{1}{2}i\gamma_R\}}. \quad (20)$$

In contrast with the case of $\omega > 2$, $(E_{1s} + \omega)$ is strictly negative (therefore $[E_k - (E_{1s} + \omega)] > 0$). It is easy to show that the above amplitude is maximum for $[E_k + E_{k'} - (E_{1s^2} + 2\omega)] = 0$ and $E_k = 0$, since these values minimize the denominator. The resulting one-electron spectrum, given by

$$\frac{dP_k}{dk} = \frac{1}{2} \int_{E_{k'}} dE_{k'} |U_{k,k'}^{(2)}(T \rightarrow \infty) + U_{k',k}^{(2)}(T \rightarrow \infty)|^2, \quad (21)$$

will show two maxima at the edges (i.e., at the excess and zero energies), corresponding to the absorption of most of the excess energy by one of the electrons while the other electron has minimum energy. This behavior of the electron energy distribution has been in fact already noticed for $\omega = 1.84$ (50 eV) [2]. It is worth noticing that neglect of γ_R in the expression of the two-photon amplitude given above would lead to a divergence as ω and E_k ($E_{k'}$) tend to 2 and 0, respectively.

Figure 2 shows the one-electron energy spectrum calculated for $\omega = 1.95$. The calculation is based on expressions (20) and (21), with $\gamma_R = \gamma_{\text{He}^+}$ (see Sec. IID). In the present case $\Delta E_R \approx 0.018$ ($n = 6$) and the condition given above, $\gamma_R \gg \Delta E_R$, is fulfilled. Incidentally we note that, at intensities of the order of 10^{12} – 10^{13} W/cm², γ_R is much smaller and the photon energy should be much closer to threshold in order to fulfill the above inequality. In practice, Eq. (15) can be used to calculate the one-electron energy spectrum. For $\omega = 2.1$ (which is the case examined in the previous section), the TPDI total probability (obtained by integrating the density of probability shown in Fig. 2) is close to 1, it is interesting to note that the double continuum is much less populated in the present case. Indeed, TPDI is now in competition with two-photon excitation-plus-ionization (TPEI) process, which dominates.

At this point it is important to discuss our approach in view of other models developed in the context of direct TPDI. It is worth noticing that, if $\gamma_R \ll \Delta E_R$, γ_R is not defined [see the remarks below Eq. (18)] and the Rydberg series plays no role. Under the latter conditions, our approach is similar to the simple model developed in [3] that ignores both correlation and screening in the final and intermediate states. The model leads to a simple expression of the differential TPDI cross section (since the TPDI probability varies linearly with T within LOPT it is appropriate to calculate cross sections); see Eq. (8) in [3]. The results agree qualitatively and quantitatively with other calculations, at least for $\omega > 1.84$ (50 eV), where it is not critical for the electrons to interact strongly in order to overcome the attraction of the nucleus [2]. In particular the model shows the U-shaped electron distribution and the rise of the TPDI probability as the photon energy increases, in agreement with TDSE results (see [2] and [7], and other references therein). The present work is complementary to previous calculations. It shows that the situation becomes

more complex for $\omega \approx 2$: close to threshold the notion of the cross section loses its pertinence; the TPDI cannot be simply expressed as a rate for given pulse parameters (intensity, wavelength, and duration), and Eq. (12) should be used to calculate the differential probability. At resonance the TPDI regime is neither direct nor sequential and there is a third open channel; the two-photon excitation-plus-ionization channel. Finally, for $\omega > 2$, we reach the sequential regime analyzed above, where the TPDI probability varies quadratically with T far from the saturation regime.

D. The sequential threshold limit ($\omega = 2$)

Finally we compare γ_R and γ_{He^+} at the threshold limit. There exists a well-known analytical expression for the radial part of the orbitals kl and nl in the region of the nucleus ($r \ll n/Z$ and $kr \ll 1$; see Bethe and Salpeter [14]),

$$R_{kl} \approx \frac{n^{3/2}}{Z} R_{nl} \quad (22)$$

with $Z = 2$ in the present case. The immediate consequence [see Eqs. (6) and (18)] is that, in the region of threshold,

$$\gamma_R \approx \gamma_{\text{He}^+}. \quad (23)$$

Considering the above equality, the similarity between Eqs. (20) and (13) is obvious. This simply demonstrates the continuity of the TPDI process, from the direct ($\omega < 2$) to the sequential ($\omega > 2$) regime.

Figure 3 shows the one-electron energy spectrum calculated at $\omega = 2$. Using negative values of E_k ($E_{k'}$), it is easy to calculate the one-electron energy spectrum associated with TPEI; it is shown in Fig. 3 for $\omega = 2$, beside the TPDI one-electron energy spectrum. Here TPDI and TPEI have equal total probability.

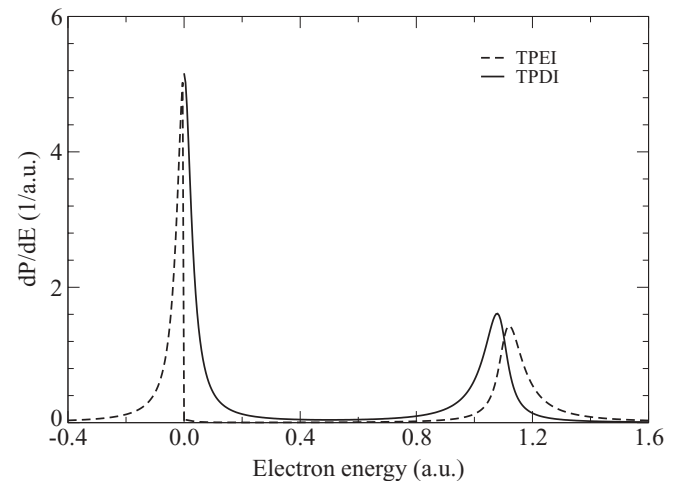


FIG. 3. TPDI and TPEI one-electron energy spectrum calculated for $\omega = 2$. The equation (15) is used with $\gamma_{\text{He}} = 0.066$ and $\gamma_{\text{He}^+} = \gamma_R = 0.061$ (see the text).

III. CONCLUSIONS

We have investigated two-photon double ionization in the region of the sequential ionization threshold. Within the given approximations, our treatment is rigorous and it takes into account all open channels, including the Rydberg state series populated through TPEI. The latter channel plays an important role. We have found a simple formula to calculate the TPDI electron spectrum in the region of threshold [Eqs. (20) and (21)]; it can be easily extended to TPEI. As the photon energy decreases from values larger than 2 to lower ones, TPDI continuously evolves from sequential to direct double ionization. In the sequential regime, the electron energy spectrum is dominated by two peaks, related to the ionization of He and He⁺. We have already noticed that the electron interaction energy ($\langle 1s^2 | 1/r_{12} | 1s^2 \rangle$ in our model) is fully transferred to the first ionized electron. A U-shaped structure emerges when the

direct regime is reached ($1.45 \ll \omega \leq 2$). In the latter case, the two-step model (ionization of He followed by the ionization of He⁺) still holds, with the difference that the first ionized electron absorbs most of the electron interaction energy, while the remaining interaction energy is transferred to the other electron. As we go “deeper” in the direct regime (e.g., with $\omega = 1.65$) the latter picture is not valid; the two electrons being emitted almost simultaneously, they strongly interact, with important consequences on the angular and energy electron distributions (see [15], and other references therein). Regarding future investigations, a more sophisticated treatment of electron correlations is certainly required in order to evaluate accurately the relative importance of the different open channels at threshold. As a matter of fact, we do not expect that correlation effects, calculated beyond the zero-order approximation, will modify the qualitative conclusions of this work.

-
- [1] H. Bachau and P. Lambropoulos, *Phys. Rev. A* **44**, R9 (1991).
 [2] E. Fomouo, Ph. Antoine, B. Piraux, L. Malegat, H. Bachau, and R. Shakeshaft, *J. Phys. B* **41**, 051001 (2008).
 [3] D. A. Horner, F. Morales, T. N. Rescigno, F. Martín, and C. W. McCurdy, *Phys. Rev. A* **76**, 030701 (2007).
 [4] R. Shakeshaft, *Phys. Rev. A* **76**, 063405 (2007).
 [5] J. Feist, S. Nagele, R. Pazourek, E. Persson, B. I. Schneider, L. A. Collins, and J. Burgdörfer, *Phys. Rev. A* **77**, 043420 (2008).
 [6] A. Palacios, T. N. Rescigno, and C. W. McCurdy, *Phys. Rev. A* **79**, 033402 (2009).
 [7] R. Nepstad, T. Birkeland, and M. Førre, *Phys. Rev. A* **81**, 063402 (2010).
 [8] M. Førre, S. Selstø, and R. Nepstad, *Phys. Rev. Lett.* **105**, 163001 (2010).
 [9] P. Lambropoulos, L. A. A. Nikolopoulos, M. G. Makris, and A. Mihelič, *Phys. Rev. A* **78**, 055402 (2008).
 [10] A. T. Georges and P. Lambropoulos, *Advances in Electronic and Electron Phys.* **54**(C), 191 (1980).
 [11] P. Lambropoulos and P. Zoller, *Phys. Rev. A* **24**, 379 (1981).
 [12] C. Cohen-Tannoudji, J. Dupont-Roc, and G. Grynberg, *Processus d'Interaction entre Photons et Atomes* (InterEditions/Editions du CNRS, Paris, 1988).
 [13] U. Fano, *Phys. Rev.* **124**, 1866 (1961).
 [14] H. A. Bethe and E. E. Salpeter, *Quantum Mechanics of One and Two-Electron Atoms* (Springer, Berlin, 1957).
 [15] E. Fomouo, H. Bachau, and B. Piraux, *Eur. Phys. J. Spec. Top.* **175**, 175 (2009).